Modeling of entrained flow steam gasification of sewage sludge

Jakub Mularski[1], Kamil Stasiak[2], Michał Ostrycharczyk[3], Michał Czerep[4], Mateusz Wnukowski[5], Krystian Krochmalny[6], Marcin Baranowski[7], Paweł Ziółkowski[8], Mateusz Kowal[9], Łukasz Niedźwiecki[10], Halina Pawlak-Kruczek[11], Dariusz Mikielewicz[12]

[1,3,4,5,6,7,9,10,11] Wroclaw University of Science and Technology; Wybrzeze Wyspianskiego 27, 50-370 Wroclaw, Poland
e-mail: jakub.mularski@pwr.edu.pl, michal.ostrycharczyk@pwr.edu.pl, michal.czerep@pwr.edu.pl, mateusz.wnukowski@pwr.edu.pl, krystian.krochmalny@pwr.edu.pl, marcin.baranowski@pwr.edu.pl, mateusz.kowal@pwr.edu.pl, lukasz.niedzwiecki@pwr.edu.pl, halina.pawlak@pwr.edu.pl

[4,10,11,12] Faculty of Mechanical Engineering and Ship Technology, Institute of Energy, Gdańsk University of Technology, 80-233 Gdańsk, Poland
e-mail: kamil.stasiak@pg.edu.pl, pawel.ziolkowski1@pg.edu.pl, dariusz.mikielewicz@pg.edu.pl

Abstract

Proper management of sewage sludge becomes increasingly problematic due to legal requirements aiming at diminishing environmental impact, as well as rationalizing the utilization from the point of view of logistics. Steam gasification of sewage sludge can result in very good quality of the producer gas. So far, the works have been focused on the gasification in fixed bed gasifiers. However, this does not allow to take full advantage of the effect of scale, as the scalability of fixed ed gasifiers is limited. Entrained flow gasifiers are scalable up to the order of magnitude of hundreds of megawatts, which was proven for the gasification of coal. Therefore, it seems plausible to suspect that such scalability would allow building gasifiers big enough, to work as a part of bioenergy with carbon capture and storage plants, operating in an economically feasible manner, fully utilizing the effect of scale. However, the optimized design of such units would require robust modeling. This work focuses on different models for sewage sludge steam gasification, allowing accurate predictions of the producer's gas quality. The core part of this work is a comparison between the results obtained using advanced CFD models in Fluent, as well as two different equilibrium models. Results from all the models are experimentally validated, by entrained flow steam gasification in a 3 m long reactor, with an addition of CO_2.

1 Introduction

Sewage sludge is a residue of the wastewater processing, that is biologically active and consists of water, organic matter, including dead and alive pathogens, as well as organic and inorganic contaminants such as polycyclic aromatic hydrocarbons (PAHs) and heavy metals [1–3]. Storage along with landfilling and land spreading is gradually being replaced in the EU countries by methods leading to waste stabilization and safe recycling [4]. Present concerns about global warming sparked an interest in improving the energy efficiency of existing energy infrastructure [5], effective energy storage [6], as well as novel solutions aiming at capturing produced CO_2 and its subsequent storage [7–10]. As sewage sludge is considered biomass, solutions have been proposed aiming at achieving negative CO_2 emissions [11].

Due to increasing amounts of environmental restrictions, not favorable to commonly used utilization pathways, such as landfilling [12], novel thermal processes are currently a subject of active investigation, in terms of their suitability for sewage sludge utilization as well as their applicability for other waste streams. Nowadays in Poland, there are at least 45 installations for drying the sewage sludge, mostly drum and tape dryers, as well as 12 installations using solar energy [13]. Incineration may be performed in existing incineration units (at least 11) that are based on fluidized beds (mostly) and grate furnaces [13–15]. Moreover, incineration is possible in 13 facilities of cement producers in Poland [16], as well as in Municipal Waste incineration facilities existing or being closed to commissioning in 17 different cities [17,18]. In all of these cases, logistics is critical for the economic feasibility of the solution, therefore the problem of sewage sludge is the most severe in the case of small and medium-size towns, without their own thermal utilization facility, with limited possibilities of local land-spreading. It should not be overlooked, that the state-of-the-art thermal utilization leaves the problem of ashes unresolved. However, there are emerging technologies that allow the use of ash for the production of fertilizers [19].

A significant amount of work has been performed so far on the gasification of sewage sludge. Werle reported decreased temperature and increased concentration of combustible components of syngas with an increase in the oxygen content of the sludge [20]. Schweizer et al. observed hydrogen content exceeding 40% during steam gasification of sewage sludge in a laboratory-scale fluidized bed gasifier [21]. In another work, Werle determined that the laminar flame speed increased with an increasing hydrogen content of the syngas [22]. Werle and Dudziak assessed that it is possible to use syngas from sewage sludge in spark-ignition engines [23]. However, Szwaja et al. determined that syngas from sewage sludge requires a 40% addition of methane to obtain a satisfactory performance of a spark-ignition engine [24]. In another study, Werle confirmed that increased air temperature, at the inlet of a fixed bed gasifier, resulted in an increased yield of combustible compounds during the gasification of sewage sludge [25]. Calvo et al. reported hydrogen content varying between 21.0% and 20.7% and tar content between 0.846 and 0.585 g/m^3 of syngas from gasification of sewage sludge in a simple atmospheric fluidized bed gasifier [26]. Werle and Dudziak found that tars, from gasification of sewage sludge, consisted mostly of phenols and their derivatives. Judex et al. published results from an existing sewage sludge gasification plant in Balingen and Manheim (Germany), with respective processing capacities of 1 950 t/a and 5 000 t/a of dry sewage sludge [27]. Syngas produced by fluidized bed gasifiers on average had Lower Heating Value (LHV) of 3.2 MJ/m^3 and 4.7 MJ/m3, respectively [27]. Balingen gasifier worked with an average gasification temperature of 820°C, with an average excess air ratio (λ) of 0.33, whereas the gasifier in Manheim worked with an average gasification temperature of 870°C, with an average excess air ratio (λ) of 0.28 [27]. Sewage sludge in Manheim had comparably higher carbon content (30.0 %$_{dry}$) and lower ash content (39.5 %$_{dry}$) in comparison with sewage sludge from Balingen having 16.9 %$_{dry}$ carbon and 57.0 %$_{dry}$ ash, respectively [27]. Hydrogen content was not significantly different, on average 13.1% in Balingen and 13.3% in Manheim [27]. On average higher CO content (13.8% compared to 8.1%) was measured in Manheim, whereas higher CO_2 content was measured in Balingen (16.7% compared to 13.0%) [27]. The average methane content measured in Manheim (4.2%) was roughly double the one measured in Balingen (2.1%)[27].

As regards modeling of sewage sludge gasification, the published papers reported in the literature consider mainly equilibrium modeling approaches [20,28–31]. For instance, Ziółkowski et al. performed mathematical modeling of fixed-bed gasification of sewage sludge [28] which utilized the concept of stoichiometric equilibrium modeling. The model results were in good agreement with experimental data.

De Andrés et al. simulated sewage sludge gasification in a fluidized bed gasifier using Aspen Plus software [30]. The model, termed non-stoichiometric, was based on the Gibbs free energy minimization. The obtained results were also in good agreement with experimental results. Seggiani et al. developed an unsteady 1-D mathematical model for the simulation of fixed-bed sewage sludge gasifier [32]. Good agreement was achieved between the experiment and the predictions.

The main novelty of the current work considers the investigation of entrained flow steam gasification of sewage sludge where both experimental and theoretical analyses are performed. The published papers reported in the literature regarding sewage sludge consider mainly fixed-bed and fluidized-bed reactors with equilibrium modeling approaches. In the current paper, as part of the theoretical investigation, a CFD model is developed and validated against the experimental results. The utilization of entrained flow steam gasification would allow obtaining good quality syngas. It would also offer practical scale-up possibilities, thus making efficient power plants with negative CO_2 emissions possible in practice.

2   Materials and methods

The research was performed using dried sewage sludge from the Janówek wastewater treatment plant, treating wastewater from Wrocław municipality, Poland. Dried sewage sludge was milled and subsequently sieved, using a set of calibrated sieves, to determine the particle size distribution of the sample. Proximate analysis was performed using TGA/DT Pyris Diamond from Perkin Elmer. A two-step program was set, i.e. sample was heated in Nitrogen up to 105 °C with a ramp of 20°C/min, with a hold period of 15 minutes afterward. During the second step, the sample was heated up to 900 °C with a ramp of 50 °C/min, with a hold period of 15 minutes afterward. Ash content was determined using the standard gravimetric method for coal, by ashing samples at 815 °C for 3 hours. A higher heating value (HHV) was determined using IKA 3000 bomb calorimeter, using the isoperibolic method. Ultimate analysis was performed using Perkin Elmer 2400 analyzer, according to polish standard PKN-ISO/TS 12902:2007.

Experimental gasification in entrained flow was performed, using a 20 kW drop tube reactor, shown in figure 1. The reactor length is equal to 3 m, whereas the inner furnace diameter is equal to 0.135 m. Experimental parameters of gasification are shown in table 1. Results of proximate and ultimate analysis of sewage sludge, used as the feedstock, are shown in table 2.
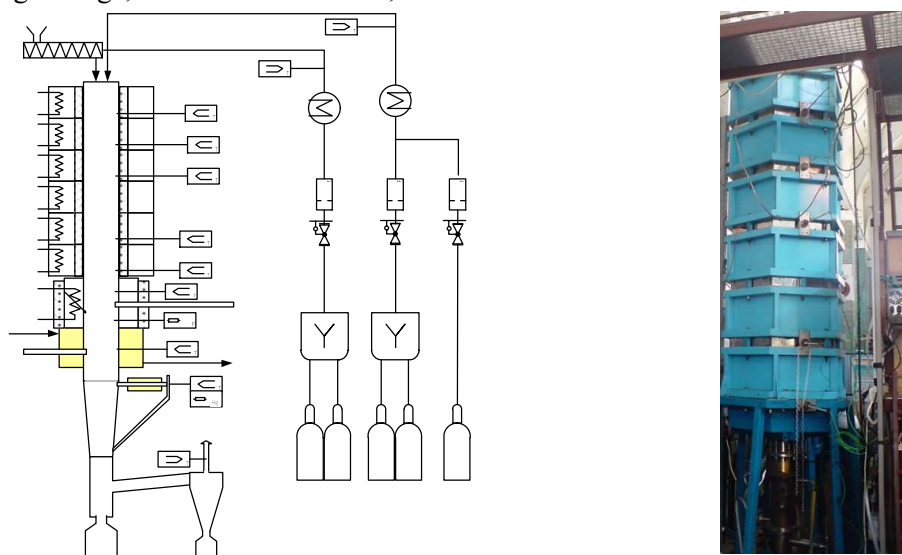

Figure 1: Isothermal flow reactor: diagram (left) and photo (right)

Table 1: Experiments parameters for gasification

Gasification temperature	1473 K
Fuel mass flow rate	2 kg/h
CO_2 volumetric flow rate	1.4 m_N^3/h
H_2O mass flow rate	0.213 kg/h

Table 2: Sewage Sludge properties

Moisture (raw)	3.43%
Ash (dry-basis)	26.4%
Volatile matter (dry-basis)	58.2 %
Char (dry-basis)	15.4 %
HHV(dry-basis)	16.62 MJ/kg
C (dry-basis)	37.71 %
H (dry-basis)	4.16 %
S (dry-basis)	1.77 %
N (dry-basis)	3 %

During the gasification experiment, tars were captured in a series of 3 impinger bottles with analytical grade isopropanol immersed in a cooling bath at the temperature of -15°C. The content of the impinger bottle was subsequently mixed and analyzed using GC-MS (gas chromatography-mass spectrometry) that consisted of the Agilent 7820-A chromatograph (manufactory, Agilent Technologies, Palo Alto, CA, USA) and the Agilent 5977B MSD spectrometer (Agilent Technologies, Palo Alto, CA, USA). In the chromatograph, the HP-5 MS column (Agilent Technologies, Palo Alto, CA, USA) was used. Helium was used as carrier gas (1.5 mL/min). A heating program was set to achieve 50°C in 5 min, subsequently heating up the column with a ramp of 10°C/min until the temperature of 250°C was reached and held for another 10 min. Finally, the oven was heated up to 300°C and held in it for 20 min. The applied split was 40. The produced gas obtained during gasification was measured with the use GAS 3000 SYNGAS analyzer (Atut, Lublin, Poland) to determine the content of H_2, CO, CO_2, and CH_4.

2.1 CFD modeling of sewage sludge gasification

The modeling framework for combustion/gasification processes of solid fuels, such as coal, or biomass (e.g. sewage sludge), despite different fuel physicochemical properties, remains the same. It is because these fuels undergo the same global combustion/gasification steps:

- Inert heating
- Drying
- Devolatilization
- Gas-phase reactions
- Char conversion

For example, in [33–35], the same drying, devolatilization, gas-phase, and char conversion models have been used for biomass gasification as for coal combustion/gasification studies [36,37]. The main difference considered the kinetic parameters of these models. The relative difference between coal and biomass kinetic parameters values corresponded to different fuel properties, and operating conditions. The distinctive biomass structure, particle morphology, and different physicochemical properties are, unfortunately, not explicitly considered in the commonly applied global models. But these factors have a direct effect on the strength and time scale of the aforementioned combustion steps. Moreover, due to fuel differences, the advanced phenomenological coal mechanisms may not be suitable for biomass, specifically, for sewage sludge. Therefore, in the current paper, global empirical approaches were incorporated.

The mathematical model applied to study entrained flow sewage sludge gasification is based on the commercial software Ansys Fluent 2021R2 [38]. The gas phase is modeled using an Eulerian approach. The trajectories of the discrete phase are calculated applying a Lagrangian formulation and the coupling between the phases is accounted for through particle sources of Eulerian gas-phase equations [39]. The following processes are simulated inside the drop tube furnace: turbulent flow, moisture evaporation, devolatilization, gas-phase reactions, surface reactions, and radiative and particle transport. Turbulence is modeled with the realizable k-ε approach [40]. Turbulent dispersion of particles is accounted for with a stochastic tracking model [41]. Radiation is modeled with the advanced discrete ordinate method [38]. Devolatilization is modeled with the competing two-step (C2SM) reaction mechanism [42] where one

of the reactions predominates at lower heating rates, whereas the other at higher heating rates. Gas-phase reactions were modeled with the global approach, whereas turbulence-chemistry interaction was accounted for with the eddy dissipation concept (EDC)[43][44]. For char conversion, the kinetics/diffusion-limited model was applied [45]. A summary of applied models and made assumptions are presented in Table 3. Kinetic parameters for the corresponding models are presented in Table 4.

Table 3: Summary of applied models and main assumptions

Models	
Devolatilization:	Competing two-step reaction mechanism (C2SM) [42]
Gas phase:	Global reaction approach with eddy dissipation concept [43][44]
Char conversion:	Kinetics-diffusion model [45]
Turbulence:	Realizable k-ε model [40]
Radiation:	Discrete ordinate method [38], Weighted sum of gray gas model [38]
Particle tracking:	Discrete phase model, Discrete random walk model [41]
Pressure-velocity coupling	Semi-implicit method for pressure linked equations (SIMPLE) [46]
Main model assumptions	
The gasifier is operated under steady-state conditions.	
The gas phase is considered an incompressible ideal gas.	
All fuel particles are spherical, and slags during gasification are not accounted for.	
The contents of sulfur and nitrogen and associated reactions are neglected.	

Table 4: Kinetic parameters of devolatilization reaction, gas-phase, and surface reactions.

Reactions:	**Kinetic parameters: A – kg/s Pa, E- J/kmol, α- no unit**
Devolatilization:	
$Volatiles \rightarrow 0.501C_6H_5OH + 0.045H_2 + 0.036CH_4 + 0.024CO$ $+ 0.132CO_2 + 0.007C_2H_4 + 0.007C_2H_6 + 0.007C_3H_8$ $+ 0.242H_2O$	$A_1 = 2 \times 10^5$ $E_1 = 1.046 \times 10^8$ $\alpha_1 = 0.3$ $A_2 = 1.3 \times 10^7$ $E_2 = 1.674 \times 10^8$ $\alpha_2 = 1$ [47,48]
Gas-phase reactions:	
$C_6H_5OH + 5H_2O \rightarrow 6CO + 8H_2$	$A = 3 \times 10^8$ $E = 1.26 \times 10^8$ [49]
$C_mH_n + H_2O \rightarrow mCO + \left(\frac{n}{2} + 1\right)H_2$	$A = 3 \times 10^8$ $E = 1.26 \times 10^8$ [49]
$CO + H_2O \rightarrow CO_2 + H_2$	$A = 2.75$ [46] $E = 8.38 \times 10^7$ [50]
Surface reactions:	
$C(s) + CO_2 \rightarrow 2CO$	$A = 0.3$ $E = 2.00 \times 10^8$ [51]
$C(s) + H_2O \rightarrow CO + H_2$	$A = 0.002$ $E = 1.96 \times 10^8$ [51]

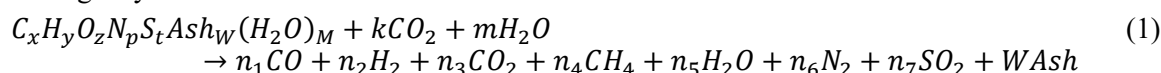Where C_mH_n in Table 4 stands for CH_4, C_2H_4, C_2H_6, and C_3H_8.

It was assumed that the reaction kinetics of C_6H_5OH and C_mH_n with H_2O is similar to the kinetics of light hydrocarbon molecules, such as CH_4 [49]. The choice is justified because these reaction rates do not vary largely [50,52]. The phenol compound C_6H_5OH was considered to represent the liquid by-products (tars). The assumption was based on the experimental measurements of sewage sludge gasification and pyrolysis where phenols were the most abundant tar species [1,47]. The complete devolatilization gas products are assumed based on [47].

The particle size follows a Rosin-Rammler distribution. The parameters used in this work are as follows: the minimum, mean and maximum diameters are 25, 200, and 813 μm, respectively. The spread parameter is equal to 1.1. The geometry of the reactor is discretized using a 2D axisymmetric grid composed of about 200 000 rectangular cells. The cell size is equal to 1 mm in both axial and radial directions. The SIMPLE [46] algorithm is used for pressure-velocity coupling. Second-order schemes are used for spatial discretization. The weighted-sum of gray gas (WSGG) model [38] is used for the calculation of the gas absorption coefficient.

2.2 Equilibrium models

The second modeling approach considers equilibrium calculations. There are two general approaches for equilibrium modeling: a stoichiometric equilibrium model (based on equilibrium constants of reactions) and a non-stoichiometric equilibrium model (based on the minimization of the Gibbs free energy) [53]. The present paper considers both modeling approaches.

In the stoichiometric model, the gasification process is represented by the global reaction defined in the following way:

$$C_xH_yO_zN_pS_tAsh_W(H_2O)_M + kCO_2 + mH_2O \qquad (1)$$
$$\rightarrow n_1CO + n_2H_2 + n_3CO_2 + n_4CH_4 + n_5H_2O + n_6N_2 + n_7SO_2 + WAsh$$

Where: x, y, z, p, t, W, M – molar masses of elements and components per 1 kg of feedstock in [mol·kg^{-1}], k – molar mass of CO_2 in [mol·kg^{-1}], and n_1, n_2, n_3, n_4, n_5, n_6, and n_7 – molar masses of syngas components after gasification in [mol·kg^{-1}]. Char and tar formation are neglected. Molar masses of fuel components are calculated based on the fuel ultimate analysis, whereas syngas components are calculated based on two equilibrium reactions. The first reaction (Eq.2) is a water-gas shift reaction.

$$CO + H_2O \rightarrow CO_2 + H_2 \qquad (2)$$

The equilibrium constant is equal to:

$$K_1 = \frac{f_{H_2} \times f_{CO_2}}{f_{CO} \times f_{H_2O}} \qquad (3)$$

Where $f_{CO}, f_{H_2O}, f_{H_2}, f_{CO_2}$ – mole fractions of CO, H_2O, H_2, and CO_2 in [% mol]. And the second reaction:

$$C(s) + 2H_2 \rightarrow CH_4 \qquad (4)$$

The equilibrium constant for the second reaction is equal to:

$$K_2 = \frac{f_{CH_4}}{f_{H_2}^2} \times \frac{1}{p} \qquad (5)$$

Where f_{CH_4}, f_{H_2} – mole fractions of CH_4 and H_2 in [% mol], p – operating pressure in [atm]. Mole fraction of the particular compound f_i is defined in the following way:

$$f_i = \frac{n_i}{\sum_1^7 n_i} \qquad (6)$$

Equilibrium constant K is also a temperature function and is related to the standard Gibbs free energy change of reaction in the subsequent way: $ln(K) = -\frac{\Delta G^0}{RT^2}$

Therefore, for the two applied equilibrium reactions, equilibrium constants will take the following form:

$$ln(K) = \frac{-\Delta G^0}{RT_0} + \frac{-\Delta A}{R}\left(\frac{1}{T_0} - \frac{1}{T}\right) + \frac{-\Delta B}{R} ln\left(\frac{T}{T_0}\right) + \frac{-\Delta C}{R}(T - T_0) + \frac{-\Delta D}{2R}(T^2 - T_0^2) \qquad (7)$$
$$+ \frac{-\Delta E}{3R}(T^3 - T_0^3)$$

Where $\Delta A_i, \Delta B_i, \Delta C_i, \Delta D_i,$ and $\Delta E_i,$ are calculated for the two equilibrium reactions. For example, $\Delta A_1 = A_{CO} + A_{H2O} - A_{CO2} - A_{H2}$. The $A_{CO}, A_{H2O}, A_{CO2},$ and A_{H2} parameters are the regression coefficients taken from [54]. Ultimately, based on energy and mass balances, and equilibrium relations, a system of equations is solved that allows obtaining the unknown syngas components after the gasification process.

In the second modeling approach, the Cycle-Tempo software [55] was used to predict the chemical equilibrium gas composition through the minimization of Gibbs free energy. This approach is termed non-stoichiometric due to the absence of any specific chemical reaction. Elemental composition determined from ultimate analysis is the only input required to the model. This approach is particularly suitable for gasification modeling since all the reactions that can occur during gasification are not fully known.

3   Results and discussion

Fig. 2 illustrates the temperature distribution, CO, H_2, CO_2, and H_2O mole fraction distributions inside the drop tube from the CFD model. Due to no oxygen presence at the inlet, and no oxidation reactions, the gasification reactions with CO_2 and H_2O dominate. The process is allothermal which means that external energy in the form of heat is provided to initiate gasification reactions as there is no oxygen supply. A gradual increase in CO content along the drop tube can be observed indicating a reasonable reactor length for the gasification reactions to convert the solid feedstock into a combustible gas product. At the same time, a gradual decrease in CO_2 content can be noticed indicating a constant utilization of CO_2 as a gasifying agent. Fig. 3 presents the product gas composition concerning the experiment, CFD model, and the equilibrium approach. One can observe a close agreement of CO and CO_2 mole fraction species between the CFD model and the experiment. The H_2 content has been overpredicted by the CFD model by 10%. The CO content was underpredicted by 7%, while the CH_4 concentration and CO_2 concentration matched the experimental data. One of the reasons for the misprediction with respect to CO and H_2 may be the initial assumption of the content of devolatilization gas products. In the modeling part of the study, tars are represented by the most basic phenol species – C_6H_5OH, whereas in the experimental studies [47], tars consisted also of amides, amines, aromatic hydrocarbons, cholestanes, cholestanols, esters, indoles, ketones, nitriles, pyridines, pyrazoles, and some other unknown species. The decomposition of these species due to reaction with H_2O will result in a different share of CO and H_2 products than in the case of pure C_6H_5OH. Moreover, the literature experiment was carried out for pyrolysis at the furnace temperature of 500°C. It is well known that devolatilization strongly depends on the heating rate and operating temperatures. Therefore, the actual gas composition after devolatilization will surely be different under high heating rate conditions. High temperatures favor tar cracking and light gas production.

The stoichiometric equilibrium model fails to predict the output gas composition indicating that the two considered gasification reactions - Eq. 2 and Eq. 4 are not in equilibrium conditions. So high prediction of CO and H_2 at the outlet, with almost no CO_2 suggests that the feedstock was entirely gasified in the model. The gasification reaction with H_2 – Eq. 4 is several orders of magnitude slower than other heterogeneous reactions, therefore, the current gasifier residence times are too small for this reaction to reach equilibrium. The non-stoichiometric equilibrium model (Cycle-Tempo) yields a better agreement with experimental data than the stoichiometric equilibrium approach. The CO concentration is overpredicted by 12%, H_2 concentration is overpredicted by 9%, and the CO_2 concentration is underpredicted 13%. The model does not predict any unconverted char at the outlet. It may be one of the reasons why there is a higher CO content and a lower CO_2 content than in the experiment. It was

also reported by other literature that the default Cycle tempo gasification module strongly underpredicts CH_4 outlet content and neglects the residual char that could be unconverted [56]. For example, in the current CFD model, the carbon conversion degree was equal to 78% for the given reactor conditions and fuel properties.
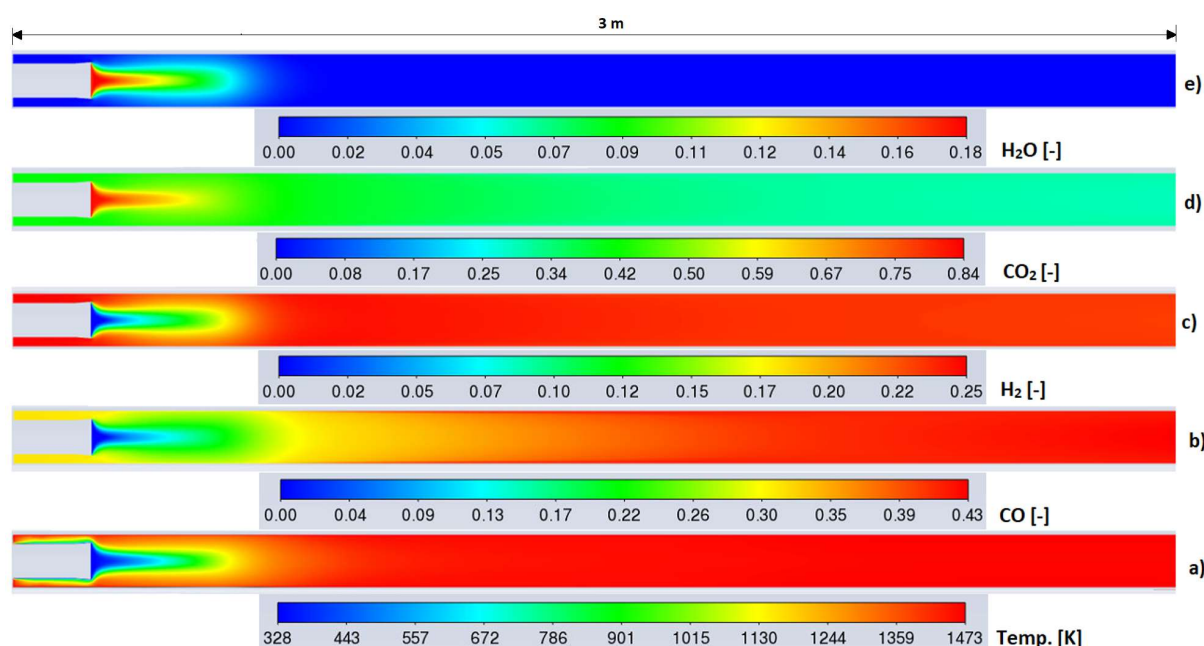

Figure 2: a) Temperature distribution, b) CO mole fraction, c) H_2 mole fraction, d) CO_2 mole fraction, e) H_2O mole fraction distribution inside a 3-meter drop tube furnace from CFD model.
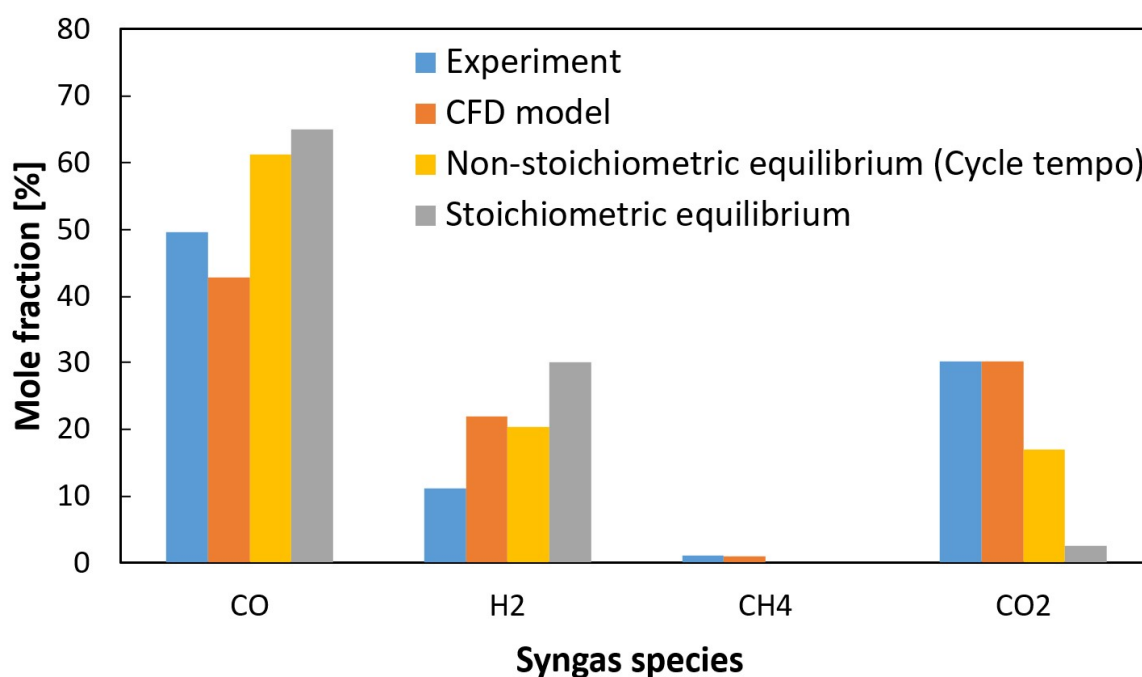
Figure 3: Product gas composition concerning experiment, CFD model, and two equilibrium models.

The tar analysis with the use of GC-MS revealed a negligible amount of tars. The BPI (base-peak ion) chromatogram showed no peaks that could be attributed to tar compounds. A more detailed analysis of two typical tar representatives, i.e., toluene and naphthalene, proved this observation. The response of naphthalene ions, if present, was merged with the background noise. The concentration of toluene was determined to be ca. 5 mg/m^3. However, this result was below the range of the calibration curve (which

was 17 mg/m^3) and might be burdened with a significant error. Regarding modeling of tars, additional work is recommended, both on the composition of primary products during pyrolysis stage, which has influence on the results obtained from secondary gas phase reactions, as suggested by Wojnicka, Ściążko and Schmid [57]. From the perspective of CFD modeling of such process in ANSYS Fluent, primary products are of special interest, since their estimated composition along with devolatilization kinetics is required as input data for the model.

4 Conclusions

It can be concluded that the CFD model has given results much closer to the experiment, in comparison to the equilibrium models, confirming its applicability for the modeling of sewage sludge gasification. It seems plausible to attribute the greater results misprediction of the equilibrium models to the fact that they have more ideal reactor operating assumptions. For example, these models neglect the unconverted char, thereby increasing the CO content and decreasing the CO_2 content according to the Boudouard reaction. The CFD model analysis has indicated that the concentration of H_2 in the reactor stabilized relatively fast, whereas a much higher length of the drop tube was needed for CO and CO_2 concentrations to stabilize, mostly due to heterogeneous reactions. The biggest advantage of steam gasification in such high temperatures is the relatively low content of tars.

Future work will be focused on the improvement of the CFD model by accounting for different tar compounds and the subsequent decomposition reactions in the devolatilization model. As opposed to coal, devolatilization gains significance in sewage sludge gasification, due to relatively high volatile matter content and low char content. The decomposition of multiple different tar species due to reaction with H_2O or other gasifying agents will result in a slightly different share of CO and H_2 products than in the case of pure C_6H_5OH (phenol) as a single tar species. It will be a huge step forward for the reliable prediction of the syngas composition from the CFD model of sewage sludge gasification.

References

[1]   Werle S, Dudziak M. Analysis of organic and inorganic contaminants in dried sewage sludge and by-products of dried sewage sludge gasification. Energies 2014;7:462–76. https://doi.org/10.3390/en7010462.

[2]   Kacprzak M, Neczaj E, Fijałkowski K, Grobelak A, Grosser A, Worwag M, et al. Sewage sludge disposal strategies for sustainable development. Environ Res 2017;156:39–46. https://doi.org/10.1016/j.envres.2017.03.010.

[3]   Lee LH, Wu TY, Shak KPY, Lim SL, Ng KY, Nguyen MN, et al. Sustainable approach to biotransform industrial sludge into organic fertilizer via vermicomposting: a mini-review. J Chem Technol Biotechnol 2018;93:925–35. https://doi.org/10.1002/jctb.5490.

[4]   Cieślik BM, Namieśnik J, Konieczka P. Review of sewage sludge management: Standards, regulations and analytical methods. J Clean Prod 2015;90:1–15. https://doi.org/10.1016/j.jclepro.2014.11.031.

[5]   Muszyński T, Andrzejczyk R, Park IW, Dorao CA. Heat transfer and pressure drop characteristics of the silicone-based plate heat exchanger. Arch Thermodyn 2019;40:127–43. https://doi.org/10.24425/ather.2019.128294.

[6]   Andrzejczyk R, Kowalczyk T, Kozak P, Muszyński T. Experimental and theoretical study of a vertical tube in shell storage unit with biodegradable PCM for low temperature thermal energy storage applications. Appl Therm Eng 2021;183. https://doi.org/10.1016/j.applthermaleng.2020.116216.

[7]   Gładysz P, Stanek W, Czarnowska L, Węcel G, Langørgen Ø. Thermodynamic assessment of an integrated MILD oxyfuel combustion power plant. Energy 2017;137:761–74. https://doi.org/10.1016/j.energy.2017.05.117.

[8]   Gładysz P, Stanek W, Czarnowska L, Sładek S, Szlęk A. Thermo-ecological evaluation of an integrated MILD oxy-fuel combustion power plant with CO2 capture, utilisation, and storage – A case study in Poland. Energy 2018;144:379–92. https://doi.org/10.1016/j.energy.2017.11.133.

[9]   Qvist S, Gładysz P, Bartela Ł, Sowiżdżał A. Retrofit Decarbonization of Coal Power Plants—A Case Study for Poland. Energies 2020;14:120. https://doi.org/10.3390/en14010120.

[10]   Gladysz P, Sowizdzal A, Miecznik M, Hacaga M, Pajak L. Techno-economic assessment of a combined heat and power plant integrated with carbon dioxide removal technology: A case study for central Poland. Energies 2020;13. https://doi.org/10.3390/en13112841.

[11]   Ziółkowski P, Madejski P, Amiri M, Kuś T, Stasiak K, Subramanian N, et al. Thermodynamic Analysis of Negative CO2 Emission Power Plant Using Aspen Plus, Aspen Hysys, and Ebsilon Software. Energies 2021;14:6304. https://doi.org/10.3390/en14196304.

[12]   Werle S, Wilk RK. A review of methods for the thermal utilization of sewage sludge: The Polish perspective. Renew Energy 2010;35:1914–9. https://doi.org/10.1016/j.renene.2010.01.019.

[13]   Werle S. Sewage Sludge-To-Energy Management in Eastern Europe: A Polish Perspective. Ecol Chem Eng S 2015;22:459–69. https://doi.org/10.1515/eces-2015-0027.

[14]   Pajak T. Thermal Treatment as sustainable sewage sludge management. Environ Prot Eng 2013;39:41–53. https://doi.org/10.5277/EPE130205.

[15]   Jurand Bień. Zagospodarowanie komunalnych osadów ściekowych metodami termicznymi. Inżynieria i Ochr Środowiska 2012;15:439–50.

[16]   Bień J, Bień B. Utilisation of Municipal Sewage Sludge By Thermal Methods in the Face of Storage Disallowing. Inżynieria Ekol 2015;45:36–43. https://doi.org/10.12912/23920629/60592.

[17]   Jurczyk MP, Pajak T. Initial Operating Experience with the New Polish Waste-to-Energy Plants. In: Karl J. Thomé-Kozmiensky, Thiel S, editors. Waste Manag., Neuruppin: TK Verlag; 2016.

[18]   Cyranka M, Jurczyk M, Pajak T. Municipal Waste-to-Energy plants in Poland – current projects. Web Conf SEED 2016 2016;10:1–8. https://doi.org/10.1051/e3sconf/20161000070.

[19]   Gorazda K, Tarko B, Wzorek Z, Kominko H, Nowak AK, Kulczycka J, et al. Fertilisers production from ashes after sewage sludge combustion – A strategy towards sustainable development. Environ Res 2017;154:171–80. https://doi.org/10.1016/j.envres.2017.01.002.

[20]   Werle S. Sewage sludge gasification: Theoretical and experimental investigation. Environ Prot Eng 2013;39:25–32. https://doi.org/10.5277/EPE130203.

[21]   Schweitzer D, Gredinger A, Schmid M, Waizmann G, Beirow M, Spörl R, et al. Steam gasification of wood pellets, sewage sludge and manure: Gasification performance and concentration of impurities. Biomass and Bioenergy 2018;111:308–19. https://doi.org/10.1016/j.biombioe.2017.02.002.

[22]   Werle S. Numerical analysis of the combustible properties of sewage sludge gasification gas. Chem Eng Trans 2015:1021–6. https://doi.org/10.3303/CET1545171.

[23]   Werle S, Dudziak M. Evaluation of the possibility of the sewage sludge gasification gas use as a fuel. Ecol Chem Eng S 2016;23:229–36. https://doi.org/10.1515/eces-2016-0015.

[24]   Szwaja S, Kovacs VB, Bereczky A, Penninger A. Sewage sludge producer gas enriched with methane as a fuel to a spark ignited engine. Fuel Process Technol 2013;110:160–6. https://doi.org/10.1016/j.fuproc.2012.12.008.

[25]   Werle S. Impact of feedstock properties and operating conditions on sewage sludge gasification in a fixed bed gasifier. Waste Manag Res 2014;32:954–60. https://doi.org/10.1177/0734242X14535654.

[26]   Calvo LF, García AI, Otero M. An experimental investigation of sewage sludge gasification in a fluidised bed reactor. Sci World J 2013. https://doi.org/http://dx.doi.org/10.1155/2013/479403.

[27]   Judex JW, Gaiffi M, Burgbacher HC. Gasification of dried sewage sludge: Status of the demonstration and the pilot plant. Waste Manag 2012;32:719–23. https://doi.org/10.1016/j.wasman.2011.12.023.

[28]   Ziółkowski P, Badur J, Pawlak- Kruczek H, Stasiak K, Amiri M, Niedzwiecki L, et al. Mathematical modelling of gasification process of sewage sludge in reactor of negative CO2 emission power plant. Energy 2021. https://doi.org/10.1016/j.energy.2021.122601.

[29]   Migliaccio R, Brachi P, Montagnaro F, Papa S, Tavano A, Montesarchio P, et al. Sewage Sludge Gasification in a Fluidized Bed: Experimental Investigation and Modeling. Ind Eng Chem Res 2021;60:5034–47. https://doi.org/10.1021/acs.iecr.1c00084.

[30]   de Andrés JM, Vedrenne M, Brambilla M, Rodríguez E. Modeling and model performance evaluation of sewage sludge gasification in fluidized-bed gasifiers using Aspen Plus. J Air Waste Manag Assoc 2019;69:23–33. https://doi.org/10.1080/10962247.2018.1500404.

[31]   Bijesh R, Arun P, Muraleedharan C. Modified stoichiometric equilibrium model for sewage sludge gasification and its validation based on experiments in a downdraft gasifier. Biomass Convers Biorefinery 2021. https://doi.org/10.1007/s13399-021-01916-w.

[32]   Seggiani M, Puccini M, Vitolo S. Gasification of sewage sludge: Mathematical modelling of an updraft gasifier. Chem Eng Trans 2013;32:895–900. https://doi.org/10.3303/CET1332150.

[33]   Gao X, Zhang Y, Li B, Yu X. Model development for biomass gasification in an entrained flow gasifier using intrinsic reaction rate submodel. Energy Convers Manag 2016;108:120–31. https://doi.org/10.1016/j.enconman.2015.10.070.

[34]   Jahromi MY, Atashkari K, Kalteh M. Comparison of different woody biomass gasification behavior in an entrained flow gasifier. Biomass Convers Biorefinery 2021.

[35]   Hu Z, Ma X, Chen Y, Liao Y, Wu J, Yu Z, et al. Co-combustion of coal with printing and dyeing sludge: Numerical simulation of the process and related NOX emissions. Fuel 2015;139:606–13. https://doi.org/10.1016/j.fuel.2014.09.047.

[36]   Mularski J, Modliński N. Entrained flow coal gasification process simulation with the emphasis on empirical devolatilization models optimization procedure. Appl Therm Eng 2020;175:1–14. https://doi.org/10.1016/j.applthermaleng.2020.115401.

[37]   Mularski J, Pawlak-Kruczek H, Modlinski N. A review of recent studies of the CFD modelling of coal gasification in entrained flow gasifiers, covering devolatilization, gas-phase reactions, surface reactions, models and kinetics. Fuel 2020;271:1–36. https://doi.org/10.1016/j.fuel.2020.117620.

[38]   Ansys Fluent User Guide 2021.

[39]   Crowe C, Sharma MP, Stosk DE. The Particle-source-in Cell (PSI-CELL) Model for Gas-droplet Flows. J Fluids Eng 1977;99:392–332. https://doi.org/doi:10.1115/1.3448756.

[40]   Shih T-H, Liou WW, Shabbir A, Yang Z, Zhu J. A new k-ϵ eddy viscosity model for high reynolds number turbulent flows. Comput Fluids 1995;24:227–38. https://doi.org/10.1016/0045-7930(94)00032-T.

[41]   Dukowicz JK. A particle-fluid numerical model for liquid sprays. J Comput Phys 1980;35:229–53. https://doi.org/10.1016/0021-9991(80)90087-X.

[42]   Kobayashi H, Howard JB, Sarofim AF. Coal devolatilization at high temperatures. Symp Combust 1977;16:411–25. https://doi.org/10.1016/S0082-0784(77)80341-X.

[43]   Spalding DB. Mixing and chemical reaction in steady confined turbulent flames. Symp Combust 1971;13:649–57. https://doi.org/10.1016/S0082-0784(71)80067-X.

[44]   Magnussen BF, Hjertager BH. On mathematical modeling of turbulent combustion with special emphasis on soot formation and combustion. Symp Combust 1977;16:719–29. https://doi.org/10.1016/S0082-0784(77)80366-4.

[45]   Smith IW. The combustion rates of coal chars: A review. Symp Combust 1982;19:1045–65. https://doi.org/10.1016/S0082-0784(82)80281-6.

[46]   Patankar S., Spalding D. A calculation procedure for heat, mass and momentum transfer in three-dimensional parabolic flows. Int J Heat Mass Transf 1972;15:1787–806. https://doi.org/10.1016/0017-9310(72)90054-3.

[47]   Wang S, Mandfloen P, Jönsson P, Yang W. Synergistic effects in the copyrolysis of municipal

sewage sludge digestate and salix: Reaction mechanism, product characterization and char stability. Appl Energy 2021;289. https://doi.org/10.1016/j.apenergy.2021.116687.

[48]   Ansys Fluent - fluid simulation software: User guide 2020 (R2) n.d. https://ansyshelp.ansys.com/account/secured?returnurl=/Views/Secured/prod_page.html?pn=Fl uent&prodver=20.2&lang=en (accessed March 9, 2020).

[49]   Kumar M, Ghoniem AF. Multiphysics Simulations of Entrained Flow Gasification . Part II : Constructing and Validating the Overall Model. Energy & Fuels 2012;26:464–79. https://doi.org/10.1021/ef2008858.

[50]   Jones WP, Lindstedt RP. Global reaction schemes for hydrocarbon combustion. Combust Flame 1988;73:233–49. https://doi.org/10.1016/0010-2180(88)90021-1.

[51]   Ku X, Li T, Løvås T. Eulerian-lagrangian simulation of biomass gasification behavior in a high-temperature entrained-flow reactor. Energy and Fuels 2014;28:5184–96. https://doi.org/10.1021/ef5010557.

[52]   Dryer FL, Westbrook CK. Simplified Reaction Mechanisms for the Oxidation of Hydrocarbon Fuels in Flames. Combust Sci Technol 1981;27:31–43. https://doi.org/10.1080/00102208108946970.

[53]   Ferreira S, Monteiro E, Brito P, Vilarinho C. A Comprehensive Review on Biomass Gasification Modified Equilibrium Models. Adv Energy Res 2020:1–49. https://doi.org/10.37247/aer.1.2020.7.

[54]   Yaws C. Handbook of Thermodynamic Properties for Hydrocarbons and Chemicals 2009.

[55]   Cycle-Tempo Software. Delft Univ Technol 2011. www.cycle-tempo.nl.

[56]   Fortunato B, Brunetti G, Camporeale SM, Torresi M, Fornarelli F. Thermodynamic model of a downdraft gasifier. Energy Convers Manag 2017;140:281–94. https://doi.org/10.1016/j.enconman.2017.02.061.

[57]   Wojnicka B, Ściążko M, Schmid JC. Modelling of biomass gasification with steam. Biomass Convers Biorefinery 2021;11:1787–805. https://doi.org/10.1007/s13399-019-00575-2.